Lead-free Solder Material Characterization For Themomechanical Modeling

Edith S.W. Poh*, W.H. Zhu, X.R. Zhang, C.K. Wang, Anthony Y.S. Sun and H.B. Tan
United Test & Assembly Center Ltd (UTAC)
Packaging Analysis & Design Center
5 Serangoon North Ave 5, Singapore 554916
*edith_candy@sg.utacgroup.com

Abstract

Systematic mechanical characterization has been done on lead-free solder alloys, i.e., SAC105, SAC205, SAC305, SAC105Ni0.02, and SAC105Ni0.05 as promising alternatives of SnPb solder. Solder joints in service stay in high homologous temperatures that have profound effects on mechanical properties such as creep and the apparent elastic modulus. Mechanical deformation behaviors of bulk solder alloys at temperatures between 298K and 398K, as well as strain rates between 10^{-5} to 10^{-1} under isothermal conditions, have been studied for the above 5 solder alloys with a designed bulk test vehicle. Isostress loading conditions on the solders were also conducted to study creep behaviour.

Based on substantial experimental measurement results, the elastic modulus, yield stress and UTS of the various SAC solder alloys show direct relationships with Ag content at temperatures between 298K and 398K. The relationships of strain rate, temperature, Ag content and material properties were developed and material constants are presented. Basic material parameters with viscoplastic constitutive relations for solders encompassing temperature and strain rate dependence have been obtained through curve fitting with experimental data. The creep constitutive model has also been established. By implementing the developed creep or viscoplastic constitutive models of solders into FEA models, the life of an electronic package under thermal cycling and drop performance under board level drop test can be evaluated.

Material compositions such as Ag content and Ni dopant effect are also studied for their influence on mechanical properties. It was reported that Ni dopant could improve solder joint drop performance by changing the microstructure of the material.

1. Introduction

With increasing requirements for lead-free solders, the industry's research has veered towards studying the mechanical properties and behaviours of the Sn-Ag-Cu solder, particularly those with alloy composition near the eutectic point [1-4]. Such solders has proven its reliability in the area of thermal cycling and have in fact been widely used as one of the lead-free solders in SMT assembly for microelectronics. Thermal fatigue life of solder joints has been reported to increase with Ag content in Sn-xAg-Cu solders [3]. However, the exponential increase in the demand of portable products has caused growing concerns over drop reliability of these high Ag content solder joints. Recent studies show that Sn-xAg-Cu lead-free solders with low Ag content exhibited longer drop lifetimes than that with high Ag content [5]. Thermal fatigue life and drop performance are now competing factors for deciding the amount of Ag content in Sn-xAg-Cu solders. Some researches has also conclude favourably on the effect of metal dopants, such as Ni, on solder joint drop performance [4]. Such dopants are known to alter the microstructure and mechanical behaviour of Sn-Ag-Cu lead-free solder [6].

This investigation is focused on understanding the mechanical properties of lead free solder material, Sn-1Ag-0.5Cu with 200ppm Ni dopant, in particular to its sensitivity towards temperatures. Solder material properties vary with temperature and strain rate significantly [7-9]. A large number of experimental data were obtained in a series of constant strain rate and constant load tests, across temperature range of -35°C to 125°C. Tensile testing is particularly chosen as tensile stress states primarily promote solder ball failure in BGA interconnect in microelectronics. Other than temperature-dependent behaviours, composition dependence such as various Ag content and Ni dopant were also studied. Bulk samples of varying Ag and Ni dopant content in Sn-Ag-Cu solders were also subjected to tensile testings.

The eventual purpose of such tedious characterization work is to develop a reliable database, which is crucial for successful numerical simulation. There is currently few published data for Sn-Ag-Cu solders with low Ag contents. In order for simulation tools to effectively enhance product development process, reliable data input is of prime importance. Material parameters of several creep models for Sn-Ag-Cu solders and the separated elasto-plasto-creep constitutive relations are developed. These parameters with viscoplastic constitutive relations for solders are used to simulate stress/strain responses of packages or board assemblies under thermal cyclic loading for comparison and verification

2. Experiment

Bulk SAC solder specimens cast in the form of a flat dog-bone shape were used as test vehicles. Dimensions are shown in Fig. 1. The specimens were annealed in air at 100°C for 2 hours to reduce any residual stresses induced during sample fabrication. A Universal Tensile Tester was used to conduct all uniaxial isostress and isostrain experiments. Isostrain tests employed the use of an extensometer to create consistent strains in the test specimen, based on a uniform gauge length of 10mm. Fig 2 shows test setup. A thermostatic chamber was used for tests at elevated and sub-zero temperatures.

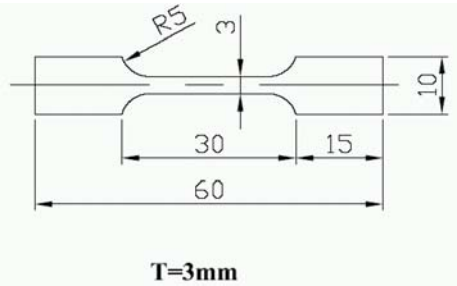

Fig. 1 Test vehicle dimensions


Fig. 2 Test setup with extensometer affixed

Fig. 3 shows typical ductile failure mode of a solder specimen after tensile loading. Surface coarsening on test vehicle display uniform deformation before the onset of highly localized deformation, a phenomenon also known as 'necking'. Total fracture usually occurs shortly after the onset of necking. Fig. 4 shows the stress-strain behaviour profile of a solder specimen which had undergone constant strain rate loading. The initial elastic part of the stress-strain curve was used to obtain the elastic modulus, achieved through curve fitting using linear relationship between stress and strain. Identical testing conditions were repeated at least twice to eliminate random errors. With good control of experimental conditions and parameters, highly repeatible test results were produced.

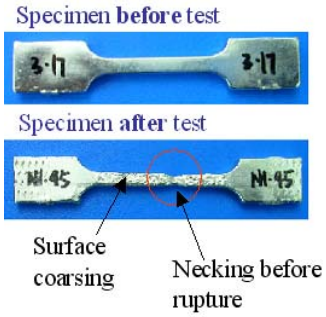

Fig. 3 Typical solder failure mode

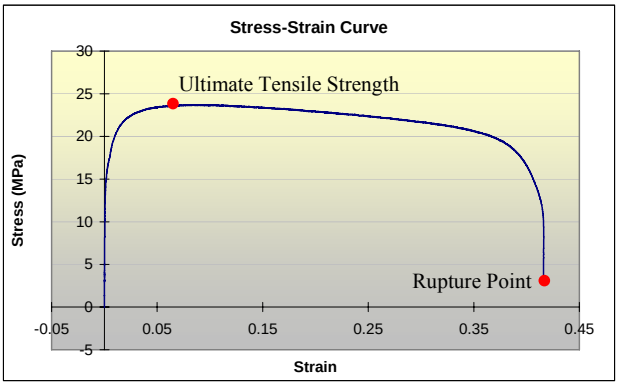

Fig. 4 Stress-strain behaviour for SAC105 under strain rate 0.01 at 75°C

Constant load testings were also conducted on the solder alloy of the different compositions to study creep behaviour. A strain vs time curve from one of the experiments presented in Fig. 5 shows distinct stages of creep behaviour. An instantaneous strain in the material is developed immediately in the primary stage of deformation, followed by the steady secondary stage. During this second phase, creep rate becomes constant and the creep strain rate can be obtained from the slope. The applied stress during this steady state plastic flow is also referred to as the saturation stress. Towards the end of the test, deformation become highly localized and accelerated at a point in the test specimen, leading to total fracture. This is known as the tertiary creep stage. As in the case of constant strain tests, identical testing conditions were repeated at least once to confirm results consistency. For low stress loading conditions, tests were not continued to complete fracture due to time factor, but stopped after steady state plastic flow was considered to have fully developed. The tests were also closely monitored and restricted to stress levels where geometric instabilities do not occur. An obvious steady state plastic flow should develop before premature strain-rate acceleration and failure.

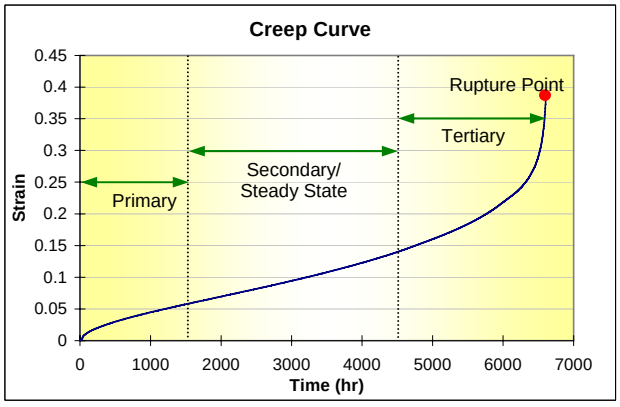

Fig. 5 Creep curve for SAC105Ni0.02 undergone isostress 20MPa at 25°C

	Tensile		Creep	
	Strain rate (1/s)	Temp (°C)	Stress (MPa)	Temp (°C)
SAC105	$10^{-1},10^{-2},10^{-3},10^{-4},10^{-5}$	25	Range from 5 - 30	25
SAC205	$10^{-1},10^{-2},10^{-3},10^{-4},10^{-5}$	25		
SAC305	$10^{-1},10^{-2},10^{-3},10^{-4},10^{-5}$	25		
SAC105Ni200ppm	$10^{-1},10^{-2},10^{-3},10^{-4},10^{-5}$	25, 75, 125, -35	Range from 5 - 30	25, 75, 125, -35
SAC105Ni500ppm	$10^{-2},10^{-3},10^{-4}$	25		

Table 1 Testing Matrix (covered in the scope of this paper)

The testing matrix covered in the scope of this paper is shown in Table 1. From the vast amount of reliable data collected, temperature effect on SAC105Ni200ppm solder mechanical behaviour is evaluated. This is particularly important as solders in service experience high homologous temperatures. Such high temperatures promote microstructural changes which leads to materials' properties variations. Ag content and Ni dopant effects in Sn-Ag-Cu solders are also discussed in detail in this paper. Further work is still on going, with results to be reported in future publications.

3. Experimental Results

3.1 Temperature effects on mechanical properties

Isostrain tensile tests conducted over a range of temperatures for SAC105Ni200ppm solder displayed high temperature sensitivity of solders. Fig. 6 showed stress-strain behaviour of SAC105Ni200ppm at temperature range of -35°C to 125°C, subjected to a constant strain rate of $0.001s^{-1}$. The solder exhibit highest yield and ultimate tensile strength (UTS) at -35°C. In this investigation, the yield stress was considered as the stress value at which 0.2% plastic strain occurs. At 125°C where it is approximately 0.8Tm of the Pb-free solder, the UTS drops to more than half of the value at -35°C. The same observations were made for the solder subjected to all other strain rates between 10^{-1} to 10^{-5}.

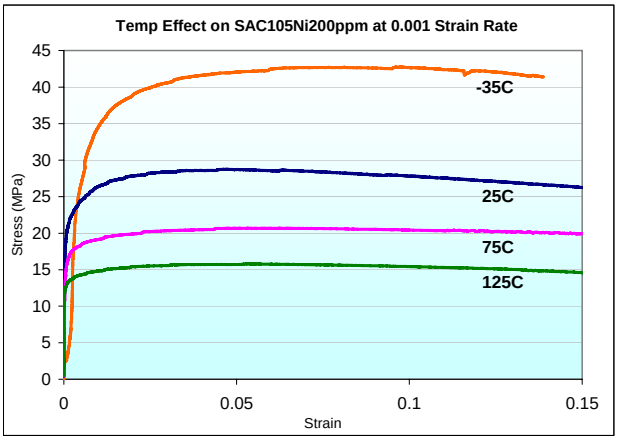

Fig. 6 Stress-strain behaviour of SAC105Ni200ppm at $0.001s^{-1}$ at different temperatures

3.2 Strain rate effect on mechanical properties

Fig. 7 shows stress-strain curves for SAC105 solder from the tensile tests of different strain rates. Strain rates are observed to affect solder material properties significantly. Yield stress and UTS increase with strain rates. After yielding, the material shows obvious ductility due to the combined creep effect. Elongation sustained by the solder before the onset of necking, or called UE in this paper, and the total elongation until catastrophic failure increase with strain rate. Fig. 8 shows material properties of modulus, yield stress, UTS, UE and total elongation of SAC105 solder with varying tensile strain rate. When tensile test was conducted under a lower strain rate, the effect of creep became more significant, leading to lower values of modulus, yield stress and UTS. Such strain rate dependent elastic modulus values obtained are also known as the apparent modulus.

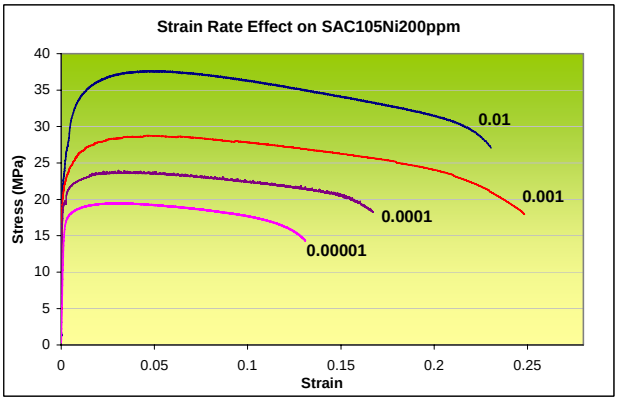

Fig. 7 Stress-strain curves of SAC105Ni200ppm at different strain rates at 25°C

From testing data analysis, the relationship between material properties and strain rate can be achieved through curve fitting. Figs. 9 – 11 show relationships of rate dependent modulus, yield stress and UTS with strain rates for SAC105 solder under room temperature testing, respectively. The graphs plotted from the experimental results show good fitting with the models. Data from other solder alloys stressed at 25°C also show good fit in similar relationships.

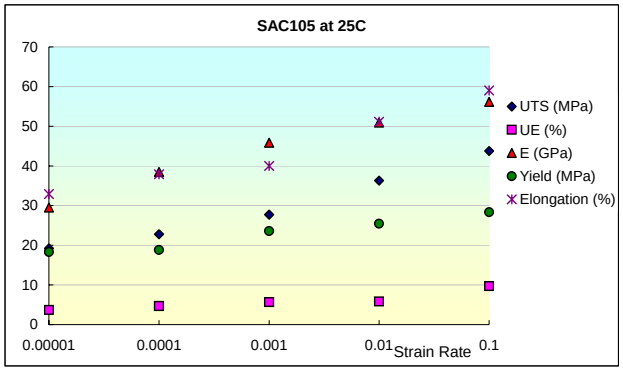

Fig. 8 Effects of strain rates on material properties of SAC105Ni200ppm at 25°C

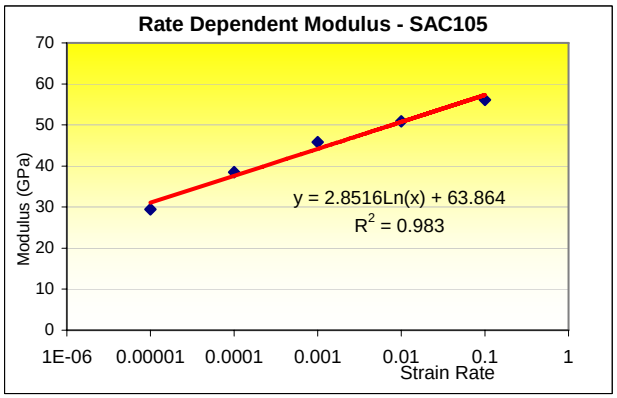

Fig. 9 Relationship between modulus and strain rates of SAC105 at 25°C

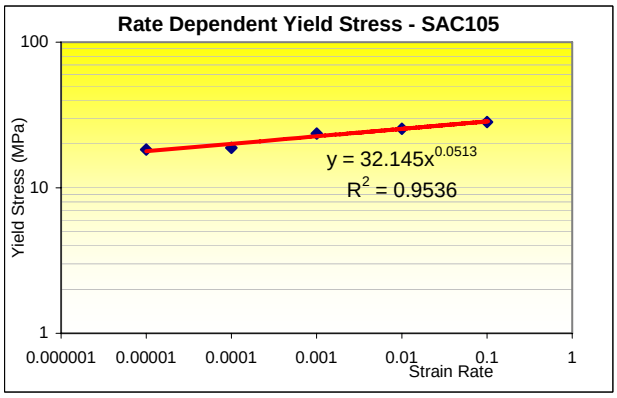

Fig. 10 Relationship between yield stress and strain rates of SAC105 at 25°C

The rate dependent modulus, yield stress and UTS satisfy the following equations,

$$E(\dot{\varepsilon})_{Sn-XAg-0.5Cu} = a_1 \log(\dot{\varepsilon}) + a_2 \quad (1)$$

$$\sigma_y(X,\dot{\varepsilon})_{Sn-XAg-0.5Cu} = b_1(\dot{\varepsilon})^{b_2} \quad (2)$$

$$UTS(X,\dot{\varepsilon})_{Sn-XAg-0.5Cu} = c_1(\dot{\varepsilon})^{c_2} \quad (3)$$

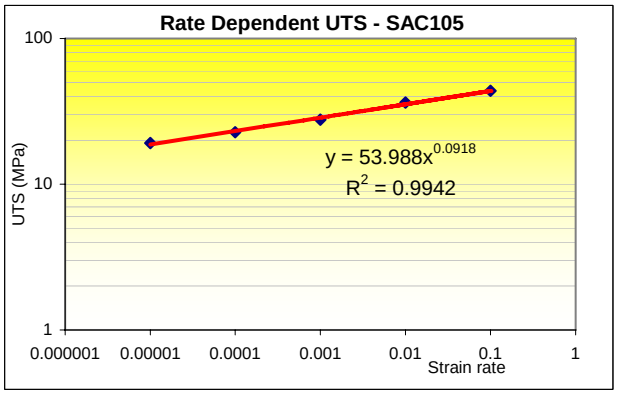

Fig. 11 Relationship between UTS and strain rates of SAC105 at 25°C

where a_1, a_2, b_1, b_2, c_1 and c_2 are material constants, which are listed in Table 2 for SAC105, SAC205, SAC305, SAC105 with 200ppm and 500ppm solders, respectively. The error between calculated material properties based on Eqs. (1) to (3) and measurement data from testing is less than 8%. The same relationships were also established for SAC105Ni200ppm for temperatures -35°C, 75°C and 125°C. The material constants are shown in Table 3.

3.3 Ag content and Ni dopant effect on solder mechanical properties

Fig. 12 – 16 show the overall effect of SAC alloy compositions on mechanical properties at different strain rates. A general trend of linear relationships can be established between Ag content and material properties. SAC solder with higher Ag content show higher strength shown by higher elastic modulus, yield stress and UTS values.

Comparing experimental data from SAC105 and SAC105Ni200ppm, Ni dopant in the solder reduces its modulus sensitivity to strain rate loadings as in Fig. 12. However, when Ni dopant is increased to 500ppm, overall apparent modulus at all strain rates decreased significantly. Further study on this solder with higher Ni doping is required for deeper understanding of this observation.

As shown in Fig. 13, 200ppm of Ni dopant in SAC105 do not significantly alter the yield stress of the solder. The effect becomes more apparent when dopant concentration increases to 500ppm. Yield stress drops drastically and losses its sensitivity to strain rates.

Fig. 14 shows very slight effect of 200ppm of Ni dopant in SAC105 solder. The drop in the ultimate tensile strength is only significant when Ni dopant increases to 500ppm.

Fig. 15 and 16 summarise deformation behaviour of all solders at all strain rates. There is a general decrease in the amount of deformation in SAC solders when Ag content increase. High Ag content in the solder reduces its overall ductility. This explains the inferior drop lifetime for electronic assembly reported by Amagai, M., et al [5], leading to the increase preference in the use of low Ag content SAC solder in packaging of portable products

Constants	a1	a2 (GPa)	b1 (MPa)	b2	c1 (MPa)	c2	Application Range
SAC105	6.57	63.86	32.15	0.0513	53.99	0.0918	0.00001 - 0.1
SAC205	5.53	65.05	38.96	0.0430	59.90	0.0746	0.00001 - 0.1
SAC305	6.00	72.43	44.00	0.0458	60.19	0.0608	0.00001 - 0.1
SAC105Ni200ppm	3.83	54.86	32.69	0.0483	65.42	0.1045	0.00001 - 0.1
SAC105Ni500ppm	10.23	65.29	16.71	0.0173	43.88	0.0960	0.0001 - 0.01

Table 2 Material Constants for Sn-xAg-0.5Cu-xNi based on Eqs (1) to (3) for strain rate effects

Constants	a1	a2 (GPa)	b1 (MPa)	b2	c1 (MPa)	c2	Application Range
25C	3.83	54.86	32.69	0.048	65.42	0.105	0.00001 - 0.1
75C	6.12	53.40	28.17	0.063	30.67	0.058	0.00001 - 0.01
125C	5.54	46.53	17.13	0.032	26.50	0.069	0.00001 - 0.01
-35C	7.04	73.92	39.18	0.050	80.38	0.085	0.0001 - 0.001

Table 3 Material Constants for Sn-1Ag-0.5Cu-0.02Ni based on Eqs (1) to (3) for strain rate effects at different temperatures

prone to drop or impact. Fig. 16 shows the amount of uniform deformation sustained by the solders before the onset of necking, or before UTS is reached. Interestingly, deformation before UTS shows a substantial jump for all solders when strain rate reaches $0.1s^{-1}$, specially for those with Ni dopant. Though strain rates experienced by solder joints during drop impact is higher than this value, this huge increase is a suggestion to why better drop performance is shown by SAC solders with low Ag content and those with Ni dopant. High Ag content in SAC solder reduces the solders' ductility, leading to lower drop lifetimes for electronic assemblies. This is consistent with the testing results by Amagai, M., et al [5]. SAC105Ni500ppm displays exceptional ability in sustaining uniform deformation before localised and accelerated deformation occurs.

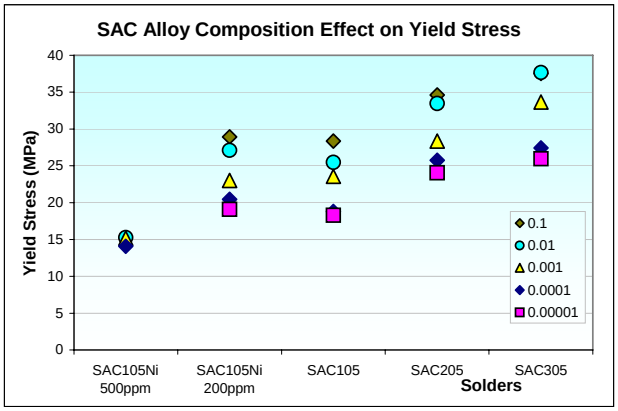

Fig. 13 SAC Alloy Composition Effect on Yield Stress at all strain rates at room temperature

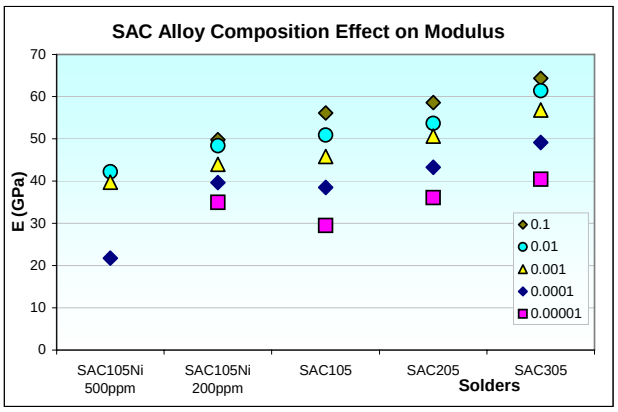

Fig. 12 SAC Alloy Composition Effect on Modulus at all strain rates at room temperature

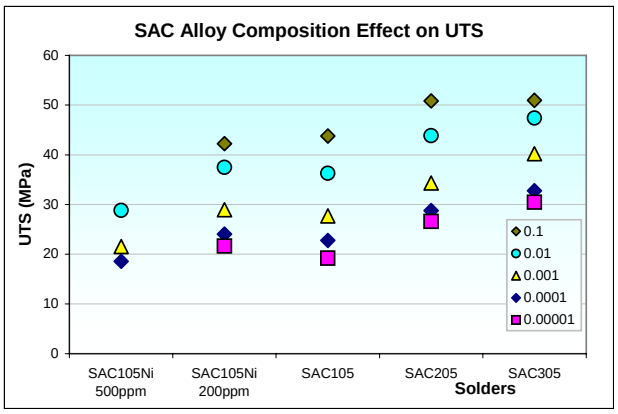

Fig. 14 SAC Alloy Composition Effect on UTS at all strain rates at room temperature

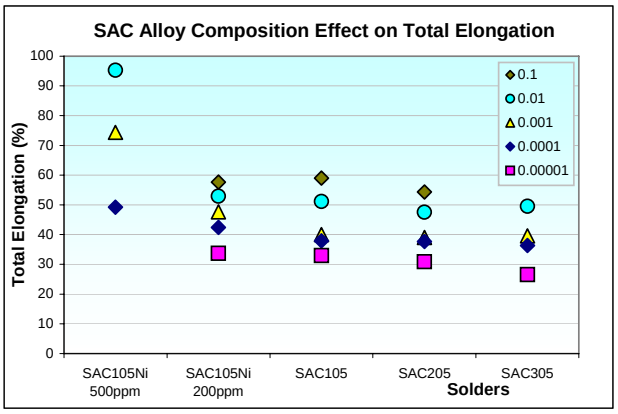

Fig. 15 SAC Alloy Composition Effect on Total Elongation at all strain rates at room temperature

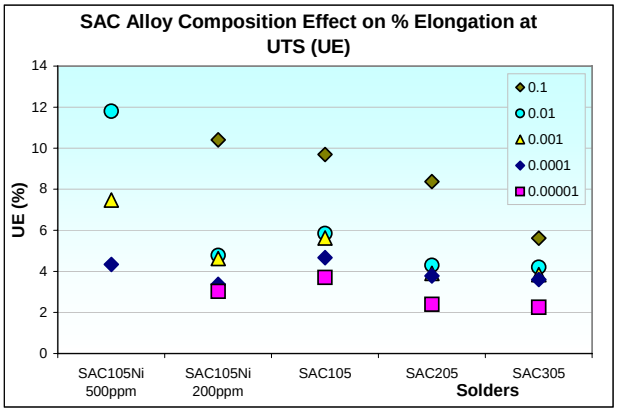

Fig. 16 SAC Alloy Composition Effect on % Elongation at UTS at all strain rates at room temperature

The relationships between Ag content in SAC solders and material properties satisfy the linear distribution model presented in Eqs. (4) to (6). Considering only testing results from Sn-Ag-Cu solders without Ni dopant, material constants were developed based on the simple relationships shown. Table 4 lists the material constants based on linear regression model for different strain rate tensile testing conditions. Table 5 compares the actual experimental and calculated values, showing good prediction.

Modulus $E = Ax + B$ (4)

Yield stress $\sigma_y = Cx + D$ (5)

$UTS = Ex + F$ (6)

Constants	A	B (GPa)	C	D (MPa)	E	F (MPa)
0.00001	5.49	24.37	3.84	15.08	5.63	14.15
0.0001	5.34	32.96	4.32	15.36	4.99	18.12
0.001	5.50	40.12	5.04	18.45	6.25	21.57
0.01	5.26	44.81	6.11	19.98	5.55	31.44
0.1	4.10	51.48	4.60	24.30	3.60	41.32

Table 4 Materials Constants for Sn-xAg-0.5Cu (without Ni dopant) solders within Ag content range of 1 – 3wt% at 25ºC (*x* is Ag content in wt%)

The above sections discuss strain rate and Ag content effect on material properties separately. Further work was done to unify both Ag content and strain rate effect on material properties. The unified Ag content and rate-dependent material property models were developed and published in a separate paper.

3.4 Temperature effects on creep behaviour

From the series of isothermal constant stress tests, creep behaviour of the SAC105Ni200ppm solder shows high sensitivity to temperature. Creep curves for SAC105Ni200ppm solder which undergone different isostress conditions at 125°C are shown in Fig. 17. Only testing data of up to 150 hours are shown. There is a general increase in secondary creep strain rates with increasing stress at all temperatures. Time to rupture naturally decreases with the increasing stress levels and temperatures.

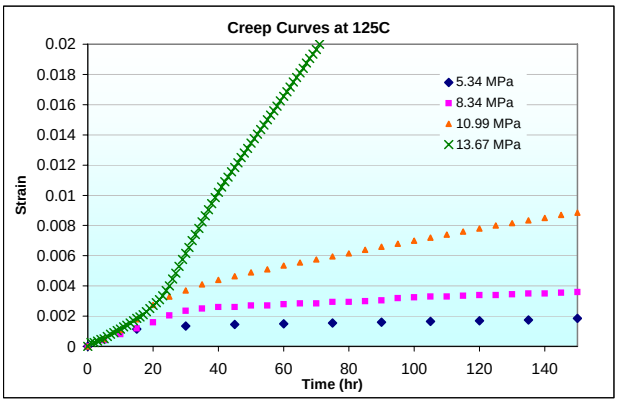

Fig. 17 Creep curves of SAC105Ni200ppm at isostress levels at 125°C (until 150 hours)

Results of this study show nonlinear characteristics, as seen from Fig. 18. Creep strain rate is observed to be less dependent on stress in the low stress regime compared to its dependence in the high stress regime.

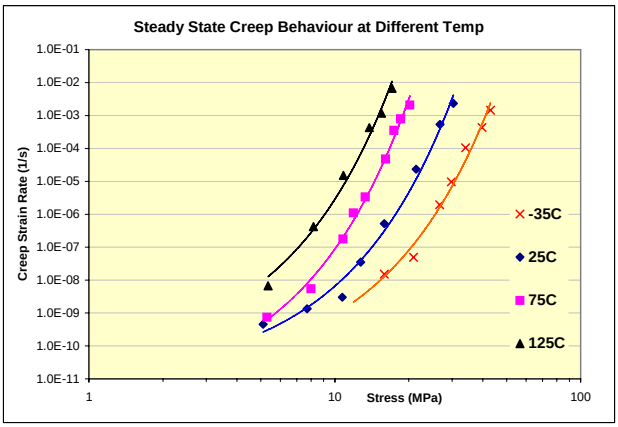

Fig. 18 Steady state creep rate of SAC105Ni200ppm at different temperatures

Strain Rate	Experimental Values			Predicted Values			Ratio (Predicted / Experimental)		
	UTS (MPa)	E (GPa)	Yield (MPa)	UTS (MPa)	E (GPa)	Yield (MPa)	UTS (MPa)	E (GPa)	Yield (MPa)
0.00001	30.45	40.47	25.96	29.89	42.45	25.97	98.2%	104.9%	100.1%
0.0001	32.75	49.15	27.44	34.38	48.45	28.86	105.0%	98.6%	105.2%
0.001	40.19	56.84	33.65	39.55	54.44	32.07	98.4%	95.8%	95.3%
0.01	47.40	61.43	37.68	45.49	60.44	35.64	96.0%	98.4%	94.6%
0.1	50.96	64.31	37.54	52.33	66.43	39.60	102.7%	103.3%	105.5%

Table 5 Comparison of actual experimental values with predicted values and percentage accuracy (Taken from testing data on SAC305 at room temperature

Non-linear curve fitting was done with the experiment data collected from isostress and isostrain tests over a range of temperatures from -35°C to 125°C for SAC105Ni200ppm. Several suitable creep models were selected for data fitting shown in Eqns. (7) – (10). Materials constant obtained are presented in Tables 6 and 7. All models are able to clearly provide acceptable descriptions of the experimental results from SAC105Ni200ppm solder.

Generalized Garofalo:

$$\dot{\varepsilon}_{Sn1Ag0.5Cu0.02Ni} = C1[\sinh(C2\times\sigma)]^{C3}\exp\left(-\frac{C4}{T}\right) \quad (7)$$

Exponential form:

$$\dot{\varepsilon}_{Sn1Ag0.5Cu0.02Ni} = C1\exp\left(\frac{\sigma}{C2}\right)\exp\left(-\frac{C3}{T}\right) \quad (8)$$

Norton form:

$$\dot{\varepsilon}_{Sn1Ag0.5Cu0.02Ni} = C1\cdot\sigma^{C2}\cdot\exp\left(-\frac{C3}{T}\right) \quad (9)$$

Coefficient	C1	C2	C3	C4
Hyperbolic-Sine	3.94e4	0.0607	6.32	7024
Exponential Form	277.42	2.11	7744	
Norton Form	2.39e-7	8.90	6283	

Table 6 Materials Constants for use in the different Creep Models

Double Power Law:

$$\dot{\varepsilon}_c = A_1\exp\left(\frac{-H_1}{kT}\right)\left(\frac{\sigma}{\sigma_N}\right)^{n1} + A_2\exp\left(\frac{-H_2}{kT}\right)\left(\frac{\sigma}{\sigma_N}\right)^{n2} \quad (10)$$

Coefficient	A1 (K/s-1)	A2	n1
Double Power Law	9.87e-7	5.01e-10	7
	n2	H1/k	H2/k
	13	4883	8949

Table 7 Materials Constants for use in the Double Power Law Model

3. Microstructure Analysis

High Ag content in SAC solder increases precipitation of IMC, mainly Ag_3Sn and Cu_6Sn_5, distributed in the Sn-rich matrix. Fig. 19 shows microstructure of the Pb-free solders with different Ag content and Ni dopant before stress testings. The amount of Ag content in the solder affects the Ag_3Sn intermetallic compound dispersion and Sn grain size. The high Ag content solder alloy shows finely dispersed IMC and Sn grain sizes, which increases solder strength and exhibit good fatigue resistance, as reported by Terashima, S., et al. [4] in a series of thermal fatique tests on assemblies with high Ag content solder joints. However, this IMC dispersion and the small Sn grain size suppress plastic deformation, thus reducing energy absorption ability of the solder alloy. This leads to inferior performance of SAC solder with high Ag content in drop reliability.. The microstructure show similar grain size and structure compared to those in conventional Pb-

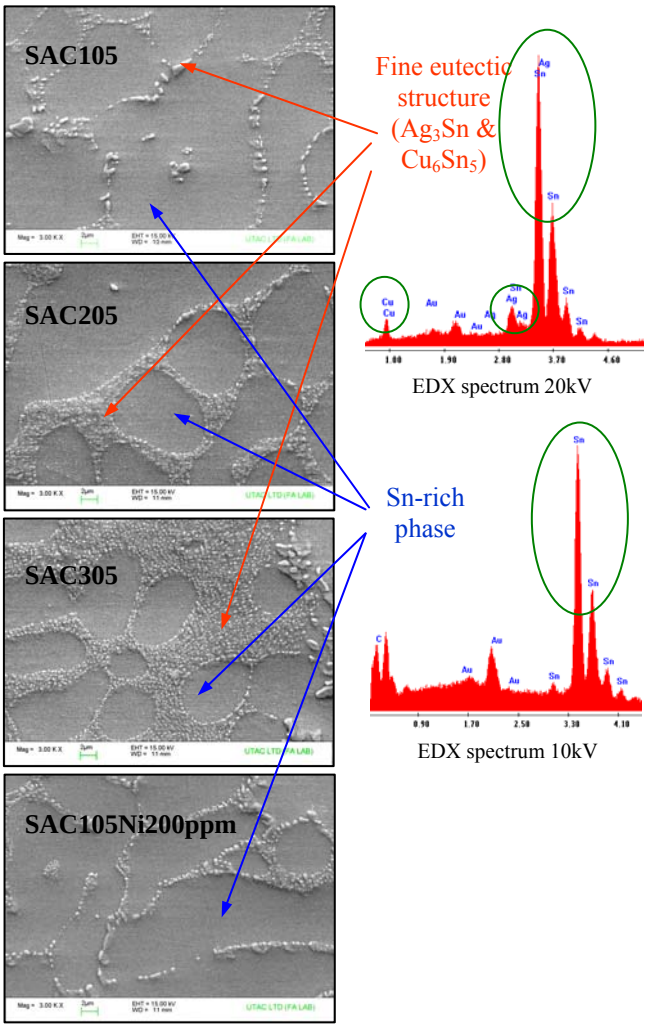

Fig. 19 SAC bulk solder microstructures

free BGA joints. This is also confirmed by Pang's investigation [2].

4. Conclusions

Isostress and isostrain tensile tests for Sn-1Ag-0.5Cu, Sn-2Ag-0.5Cu, Sn-3Ag-0.5Cu, Sn-1Ag-0.5Cu0.02Ni and Sn-1Ag-0.5Cu0.05Ni500ppm were conducted at temperatures within range of -35°C and 125°C and solder alloy composition effects, temperature effects and strain rate effects on material properties were investigated. Experimental data show high strain rates and temperature sensitivity of solders. Creep constitutive models were developed based on reliable testing data. Elongation at UTS and total elongation increase with strain rate, but decrease with Ag content due to different microstructure and IMC morphology of SAC solders. Modulus, yield stress and UTS were found to increase with strain rate and Ag content significantly. Strain rate dependent and Ag content dependent material property models were developed.

Acknowledgments

The authors would like to express their gratitude to Dr. Che Faxing previously from UTAC R&D group for advice and support for the research project, and also acknowledge the support of providing the solder bar samples from Accurus, Taiwan through its representative, PTT, Singapore.

References

1. Amagai, M., et al., "Mechanical characterization of Sn–Ag-based lead-free solders", *Microelectronics Reliability*42 (2002), pp. 951–966.
2. Pang, John H.L., et al., "Bulk solder and solder joint properties for lead free 95.5Sn-3.8Ag-0.7Cu solder alloy", *Proc 53th Electronic Components and Technology Conf*, 2003, pp. 673-679.
3. Terashima, S., et al., "Effect of silver content on thermal fatigue life of Sn-xAg-0.5Cu flip-chip interconnects", *Journal of Electronic Materials*, Vol.32 No.12 (2003), pp.1527-1533.
4. Kim, K.S., Huh, S.H.. and Suganuma, K., "Effect of fourth additive on microstructures and tensile properties of Sn-Ag-Cu alloy and joints with Cu", *Microelectronics Reliability* 43(2003), pp. 259-267.
5. Amagai, M., et al., "High Solder Joint Reliability with Lead Free Solders", *Proc 53th Electronic Components and Technology Conf* , 2003, pp. 317-322.
6. Amagai, M., "A Study of Nano Particles in SnAg-Based Lead Free Solders for intermetallic Compounds and Drop Test Performance", *Proc 56th Electronic Components and Technology Conf,* 2006, pp. 1170-1190.
7. Shi, X.Q., Zhou, W., Pang, H.L.J., and Wang, Z.P., "Effect of Temperature and Strain Rate on Mechanical Properties of 63Sn-37Pb Solder Alloy", *Journal of Electronic Packaging*, September 1999, pp. 121-179.
8. Pang, H.L.J., Xiong, B.S. and Che, F.X., "Modeling Stress Strain Curves For Lead-Free 95.5Sn-3.8Ag-0.7Cu Solder", *Proc Eurosim2004*, May 9-12, 2004, Brussels, Belgium, pp. 449-453.
9. F.X. Che*, Edith Candy Poh, W.H. Zhu, B.S. Xiong, "Ag Content Effect on Mechanical Properties of Sn-xAg-0.5Cu Solders", *Proc* 9th Electronics Packaging Technology Conference, 2007, Dec 10-12, pp. 713-718.